SIMULATION OF AN ADSORPTION COLUMN FOR THE REMOVAL OF ETHYL ACETATE FROM AIR

THIS THESIS IS SUBMITTED IN THE PARTIAL FULFILLMENT OF THE REQUIREMENT FOR THE DEGREE OF

BACHELOR OF TECHNOLOGY

In

CHEMICAL ENGINEERING

By

SHASHI SHEKHAR

(Roll No.: 110CH0383)

Under the guidance of

Dr. Basudeb Munshi

DEPARTMENT OF CHEMICAL ENGINEERING

NATIONAL INSTITUTE OF TECHNOLOGY

ROURKELA

**NATIONAL INSTITUTE OF TECHNOLOGY
ROURKELA**

<u>CERTIFICATE</u>

This is to certify that the report entitled "**SIMULATION OF AN ADSORPTION COLUMN FOR THE REMOVAL OF ETHYL ACETATE FROM AIR**" submitted by **SHASHI SHEKHAR** (Roll no.: **110CH0383**) in the partial fulfillment of the requirement for the degree of the B.Tech in Chemical Engineering, National Institute Of Technology, Rourkela is an authentic work carried out by him under my supervision. The matter embodied in the report has not been submitted to any other university/institute for any degree to the best of my knowledge.

Dr. Basudeb Munshi

Department of Chemical Engineering

National Institute Of Technology Rourkela

DECLARATION

I, Shashi Shekhar (Roll No. 110CH0383), hereby declare that this thesis is a presentation of my original work. Wherever contributions of others are involved, every effort is made to indicate this clearly, with due reference to the literature, and acknowledgement of collaborative research and discussions.

The work was done under the guidance of Dr. Basudeb Munshi at National Institute of Technology, Rourkela.

Shashi Shekhar

Department of Chemical Engineering

National Institute of Technology Rourkela

<u>ACKNOWLEDGEMENT</u>

I would like to make my deepest gratitude to Dr. B.Munshi, professor in the Department of Chemical Engineering, NIT Rourkela for giving me the opportunity to work under him and lending every support at every stage of this project work. I would also like to convey my sincerest gratitude to all the faculty members, friends and staff of the Department of Chemical Engineering, NIT Rourkela, for their invaluable support and encouragement. Lastly I would like to thank my parents for their constant support, encouragement and good wishes without which working on this project would not have been possible.

SHASHI SHEKHAR

Department of Chemical Engineering

National Institute of Technology

Rourkela

ABSTRACT

Adsorption of a toxic VOC, ethyl acetate is studied. The adsorbent used for this study is granular activated carbon. The adsorption isotherms are obtained at four distinct temperatures of 30, 35, 45, and 55° C. The physical properties of the adsorbent is provided by E-merck India. The Langmuir parameters and other data required in the simulations for this study are taken from Manjare & Ghoshal [2] [13]. The results are in agreement with that provided in Manjare & Ghoshal. The equation of state chosen for the modelling is Peng-Robinson equation of state and the momentum balance equation used is Ergun equation, best suited for both laminar and turbulent flow. The assumptions made while developing the mathematical model of the adsorption process include adiabatic and isothermal processes. The driving force is assumed to be linear. Results show that the isotherm best checks with the Langmuir isotherm model. The saturation capacity of the activated carbon varies from 0.73 to 0.487 kg/kg. The molecular diffusivity of the components is of the order of 10^{-6} m^2/s.

CONTENTS

LIST OF FIGURES

LIST OF TABLES

CHAPTER – 1

INTRODUCTION

1. INTRODUCTION

Activated carbon consists of an extensive variety of refined uncrystallised carbon-based substances. It is not in fact an amorphous material however has a micro-crystalline structure. Activated carbon has a very high porosity and an extensive particle to particle surface area. Their cooking includes two principal steps: the carbonization of the carbon-based materials at temperatures underneath 800 °C in a non-reactive environment and the activation of the carbonized material [1]. In the carbonization process, majority of the non-carbon components, e.g., oxygen (O_2), hydrogen (H_2), and nitrogen (N_2) are separated as volatile matter by the pyrolytic decay of the carbonaceous material. The remaining carbon molecules start piling up in flat, aromatic sheets connected in a haphazard manner. These random arrangements of aromatic sheets leave free interstices, which eventually develop into pores. Due to this property, activated carbons are considered among the most efficient adsorbents.

Most of the VOCs are solvents, products of physical processes like coating, gluing and drying. Ethyl acetate (EA), a vital solvent utilized in polymer and petrochemical industries, is a transparent, volatile, flammable fluid with a unique sweet smell which can be detected even at small concentrations such as 7-50 ppm. It is, in general, expelled from industries and is a major constituent of the industrial waste. To recover VOCs and to lessen their concentration in exit streams due to ecological concerns, activated carbon adsorption is employed. Many other VOCs include benzene, hexane, iso-pentane, n-heptane, propane, heptane, propylene, methylbenzene, trichloroethylene, methyl chloride, ethylene, dimethyl chloride, ethane, toluene, methane and acetone [2]. From a natural perspective, it is important to control the emission of vapours on the grounds that they influence the environmental changes, chain of growth and development of plants, people and all animals. As per a report of the National Academy of Sciences, "the arrival of Chlorofluoromethanes

like Freon-31 and chlorine-based compounds in the environment enhances the emission and absorption of IR radiation. The earth's climate and temperature are influenced, if the loss of heat from the earth is decreased. Carcinogenicity studies of specific categories of hydrocarbons demonstrate that a few cancers seem to be the result of subjection of aromatic hydrocarbons present in ash and tars [3].

Table 1. Physical Properties of Adsorbents Supplied by E-merck India [2]

Parameters	Activated Carbon *(Granular)*
Average particle diameter, mm	1.50
Pore diameter, Å	10-50
Particle bulk density, kg/m^3	500
BET surface area, m^3/g	1200
Macroporosity	0.38

1.1 REGULATION TO CONTROL VOC'S EMISSION

Regulations on controlling organic vapours in air have been an issue all around the globe. As per the regulations produced by the US Environmental Protection Agency, the maximum allowable 3-hour concentration of hydrocarbon in the ambient air is $1.6x10^{-4}$ kg/m^3 (0.24 ppm), which is not to be exceeded for over a year. VOCs react with different nitrogen oxides and other air-borne compounds, in the presence of sunlight (photo-chemically), to produce ozone, which is an essential part of smog. Under Title I of the US Clean Air Act Amendment of 1990, reduction in the release of VOCs that surpasses the current national surrounding air quality standard of 0.12 ppm for ozone is mandatory. Moreover, Title III of the amendments advocates the decrease in the emission of 189 dangerous air pollutants, the majority of which comes under the definition of VOCs [4].

The currently passed European Community stage emissions limit is 35 grams total organic compounds (35 g TOC/m3). Thus, the United States Environmental Protection Agency has made a discharge limit of 10 g TOC/m3. The German TA-Luft Standard, the most strict known fuel discharge regulation, has set an emission limit of 150 mg TOC (not methane) every cubic meter of the fuel (0.15 g TOC/m3) [4] [5] [6]. Like many under-developed nation, in India there is no discrete regulation accordingly to control VOCs discharges. On the other hand, the Clean Air Act, 1990 (Amendment) and the Factory Act, 1986 (Amendment) restrain the release/discharge of hazardous chemicals which incorporate mostly the VOCs [3].
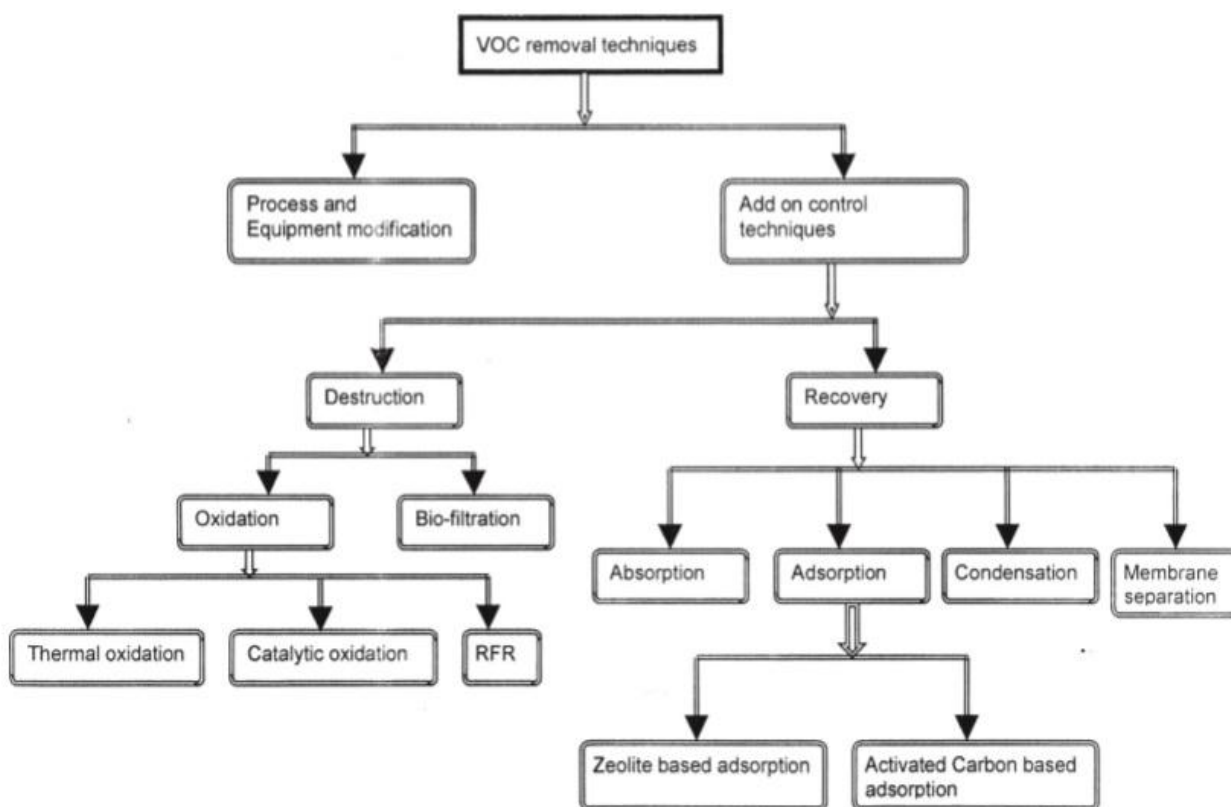

Fig 1.1: Classification of VOC control techniques

CHAPTER – 2

LITERATURE REVIEW

2. LITERATURE REVIEW

2.1 ACTIVATED CARBON

Activated carbon is a strong, permeable, dark carbonaceous material, see Fig.2.1. It is classified from basic carbon by the absence of both pollutants and an oxidized surface[7]. Any carbon source can be used to produce activated carbon using various techniques. Generally, the methodology is separated into two distinct processes carbonization and activation. In carbonization, majority of the non-carbon components are expelled in form of gas by pyrolysis of the source material. The porous surface is created during the activation process. Activation is carried out by the reaction of carbon with the activating agents. A vast majority of such agents incorporate synthetic acids, bases, and different substances in a surge of activating gasses including steam (H_2O), nitrogen (N_2) or carbon dioxide (CO_2).
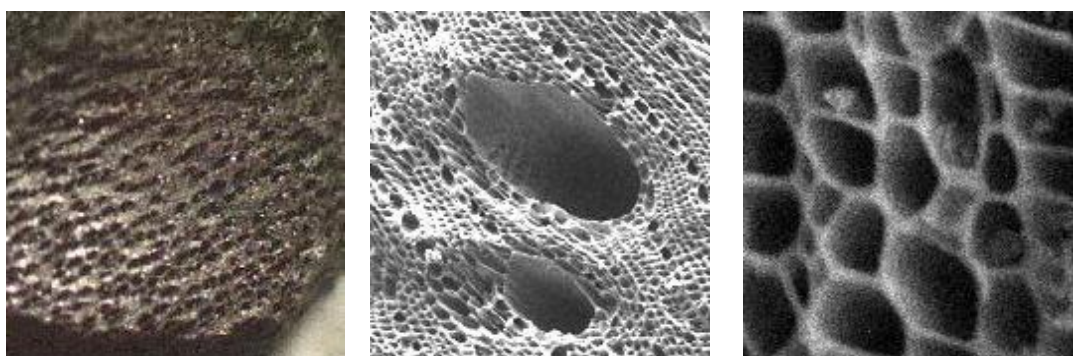
Fig 2.1: Activated carbon: pores and surface (SEM image).

Magnification increases from left to right. (Courtesy: Roplex Engineering Ltd.) [8].

Activated carbon has a remarkably enormous pore volume and surface area, making it desirable for an extensive variety of uses. It can be utilized as a purging agent, a taste and smell expelling agent or as a decolorizing agent in food industries. One vast and frequent utilization of activated carbon is in water treatment industries, including the

handling of waste and ground waters and the production of drinkable water. There are additionally various applications of activated carbon including decontamination processes in the garments, cosmetics and textile, pharmaceutical and automobile industries.

The most vital characteristic of activated carbon, the property responsible for its widespread utilization, is its pore structure. The aggregate number of pores, their size and shape decide the adsorption limit and even the rate of adsorption of the activated carbon.
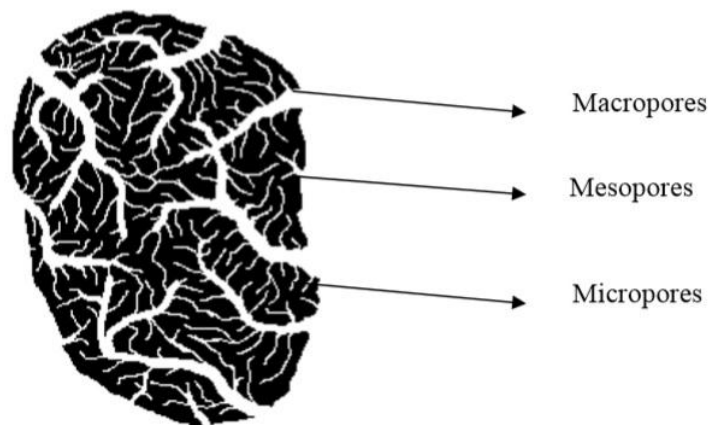
Fig 2.2: Schematic representation of different types of pores in an activated carbon.

The macropores play the role of transport media, through which the adsorbent particles go to the mesopores, after there they ultimately move into the micropores. Micropores typically comprise the biggest portion of the inner surface of the activated carbon and constitute most to the aggregate pore volume. Majority of the adsorption of gaseous adsorbates happen inside these micropores, here the forces of attraction are increased and at relatively low pressures the pores are filled.

The adsorption dynamics in the adsorption bed are affected by the size and shape of the activated carbon molecules and their impact on features of the flow. The tinier an

activated carbon molecule is, the better is the decomposition of adsorbates onto its surface and eventually the rate of adsorption is faster.

2.2 ADSORPTION

Adsorption is characterized as the improvement of material or increment in the density of the fluid (the adsorbate) in locality of an interface with a solid (the adsorbent) [9]. It might be distinguished as physisorption or chemisorption, depending upon the way of the interacting forces. In chemisorption, exchange of electrons is huge and proportionate to the arrangement of a bond between the solid surface and the sorbate.

In physisorption the interacting forces are weak relatively. Physisorption happens when an adsorbable fluid (the adsorbate) comes in physical contact with the solid surface (the adsorbent). The intermolecular forces responsible are the same as those involved in the defects of real gasses and vapour condensation [10] [11]. Moreover, the short-range repulsive forces and attractive diffusion forces, the van der Waals forces including dipole–dipole, dipole–induced dipole and induced dipole–induced dipole interactions all happen as a consequence of specific electronic and geometric properties of the adsorbent. The particles get adsorbed when the potential energy is at the very minimum [8].

Adsorption process takes place through the below mentioned steps:

o   Mass transfer – adsorbate molecules move to the outside surface of the granular activated carbon.

o   Intragranular diffusion – adsorbate molecules move inside the micropores.

o   Physical adsorption.

Thus, adsorption is dependent on: [12]

o The chemical and physical properties of the activated carbon (adsorbent).

o The chemical and physical properties of the organic vapours (adsorbate)

o The inlet adsorbate concentration.

o Physical conditions, such as relative humidity, flow velocity and temperature.

Table 2. Langmuir Parameters for adsorption of EA on Activated Carbon [13]

Temperature; K	q_s; kg/kg	b; m³/kg
303	0.73	50.92
318	0.584	41.99
328	0.487	39.58

The other isotherms available for the adsorption process include Freundlich isotherm, Langmuir-Freundlich isotherm, toth isotherm, extended Langmuir isotherm, etc. Few of the above mentioned isotherms are discussed here.

o <u>Freundlich Isotherm</u>: $q^* = K.c^n$; where K is Freundlich constant; n is Freundlich exponent.

o <u>Extended Langmuir</u>: $q^*/q_s = bc/(1 + bc)$; where q_s is saturation capacity and b is Langmuir constant.

In this thesis, the adsorption isotherm chosen for the simulation runs is Langmuir isotherm which is explained in section 3.4.

The values of saturation capacity and Langmuir constant at three distinct temperatures are provided in table 2.

CHAPTER – 3

MATHEMATICAL MODELLING

3. MATHEMATICAL MODELLING

The essential assumptions that are made while building up the mathematical model are mentioned below:

o The mixing is completely radial.

o Any axial dispersion of mass and heat is negligible.

o Air without any particulates, carbon dioxide and moisture is used as the carrier gas.

o Langmuir isotherm equation is used to represent the equilibrium relationship with Langmuir constant b, varying exponentially with temperature.

o The rate expression (driving force) of mass transfer is linear, the mass transfer coefficient used is the lumped parameter overall mass transfer coefficient.

3.1 COMPONENT MASS BALANCE: [2]

Solid phase component balance equation:

$$\frac{\partial q}{\partial t} = k(q^* - q)$$

(1)

Fluid phase component balance equation:

$$\frac{\partial c}{\partial t} = -\frac{v_o}{\epsilon}\frac{\partial c}{\partial z} - \frac{\rho_b}{\epsilon}\frac{\partial q}{\partial t}$$

(2)

3.2 ENERGY BALANCE: [2]

Solid phase energy balance equation:

$$\frac{\partial T_s}{\partial t} = \frac{(-\Delta H)\partial q}{C_{ps}\ \partial t} - \frac{ha_p}{\rho_s C_{ps}}(T_s - T_g)$$

(3)

Fluid phase energy balance equation:

$$\frac{\partial T_g}{\partial t} = \frac{ha_p}{\rho_g C_{pg}} \frac{(1-\epsilon)}{\epsilon}(T_s - T_g) - \frac{v_o}{\epsilon} \frac{\partial T_g}{\partial z} - \frac{2h_w(T_g - T_w)}{R\epsilon \rho_g C_{pg}}$$

(4)

3.3 MOMENTUM BALANCE

The momentum balance assumption in the simulations used is Ergun Equation [14] [15]:

$$\frac{\partial P}{\partial z} = -\left(\frac{1.5 \times 10^{-3}(1-\varepsilon_i)^2}{(2r_p \psi)^2 \varepsilon_i^3} \mu v_g + 1.75 \times 10^{-5} M\rho_g \frac{(1-\varepsilon_i)}{2r_p \psi \varepsilon_i^3} v_g^2 \right)$$

(5)

Ergun Equation is valid for both turbulent and laminar flow. This equation is the combination of pressure drops by Burke-Plummer equation and Karman-Kozeny equation for turbulent flow and laminar flow respectively. [14] [15]

Burke-Plummer equation [14] [15]

$$\frac{\partial P}{\partial z} = -1.75 \times 10^{-5} \frac{M\rho_g (1-\varepsilon_i)}{2r_p \psi \varepsilon_i^3} v_g^2$$

Karman-Kozeny equation [14] [15]

$$\frac{\partial P}{\partial z} = \frac{-1.5 \times 10^{-3} \mu(1-\varepsilon_i)^2}{(2r_p \psi)^2 \varepsilon_i^3} v_g$$

3.4 ADSORPTION ISOTHERM MODEL

Langmuir isotherm model are generally applied to single molecule layer adsorption on a homogenous surface. The interaction between the adsorbed molecules is negligible.

$$\frac{q^*}{q_s} = \frac{bc}{1 + bc}$$

(6)

The exponential dependence of the Langmuir constant, b on temperature is given by the van't Hoff equation: [16]

$$b = b_o e^{-\Delta H/RT}$$

(7)

The Aspen Adsim model of Langmuir isotherm equation [14] is given as:

$$w_i = \frac{IP_1 c_i}{1 + IP_2 c_i} \quad ;$$

(8)

Where w_i is the solid loading represented in kmol/kg and c_i is given in kmol/m^3.

Comparing equation (6) and (8), we get the values of IP_1 and IP_2 as given as: $IP_1 = q_s b$ / M; $IP_2 = b$ / M, where M is the molar molecular weight of the feed mixture.

3.5 DEDUCTION OF OVERALL MASS TRANSFER COEFFICIENT

Representation of most of the particle shapes as a sphere is a compulsory assumption and hence the transport can be defined by the diffusion equation written in spherical coordinate system assuming the diffusivity to be constant as: [16]

$$\frac{\partial q}{\partial t} = D_e\left(\frac{\partial^2 q}{\partial r^2} + \frac{2}{r}\frac{\partial q}{\partial r}\right)$$

(9)

Solution of the above equation using satisfactory initial conditions and boundary conditions [16] is as follows:

$$\frac{q}{q^*} = 1 - \frac{6}{\pi^2}\sum_{n=1}^{\infty}\frac{1}{n^2}\exp\left(-\frac{n^2\pi^2 D_e t}{R_p^{\,2}}\right)$$

(10)

The above equation shows rapid convergence in the long time region. This is due to the fact that the higher terms of the summation are negligibly small. On approximation, the 1st term remains intact and the rest vanishes to get: [16] [17]

$$1 - \frac{q}{q^*} \approx \frac{6}{\pi^2}\exp\left(-\frac{\pi^2 D_e t}{R_p^{\,2}}\right)$$

(11)

Differentiating equation (11) and equating with equation (1); we get a relationship between the overall mass transfer coefficient and the effective diffusivity which is given as:

$$k = 9.9\, D_e / R_p^{\,2}$$

(12)

CHAPER – 4

SIMULATION TOOL

4. SIMULATION TOOL

4.1 INTRODUCTION

Aspen Plus is a process modelling equipment for performance monitoring, design, and optimization for the coal power, metals and minerals, polymer, chemical and specialty chemical industries.

Aspen Adsim is vastly used for the simulation of gas processes involving only adsorption, or gas processes with adsorptive reactions where both adsorption and reaction take place at the same time. Gaseous-phase adsorption is extensively utilized for the bulk separation or large scale purification of natural gas, petrochemicals, air and chemicals. [14]
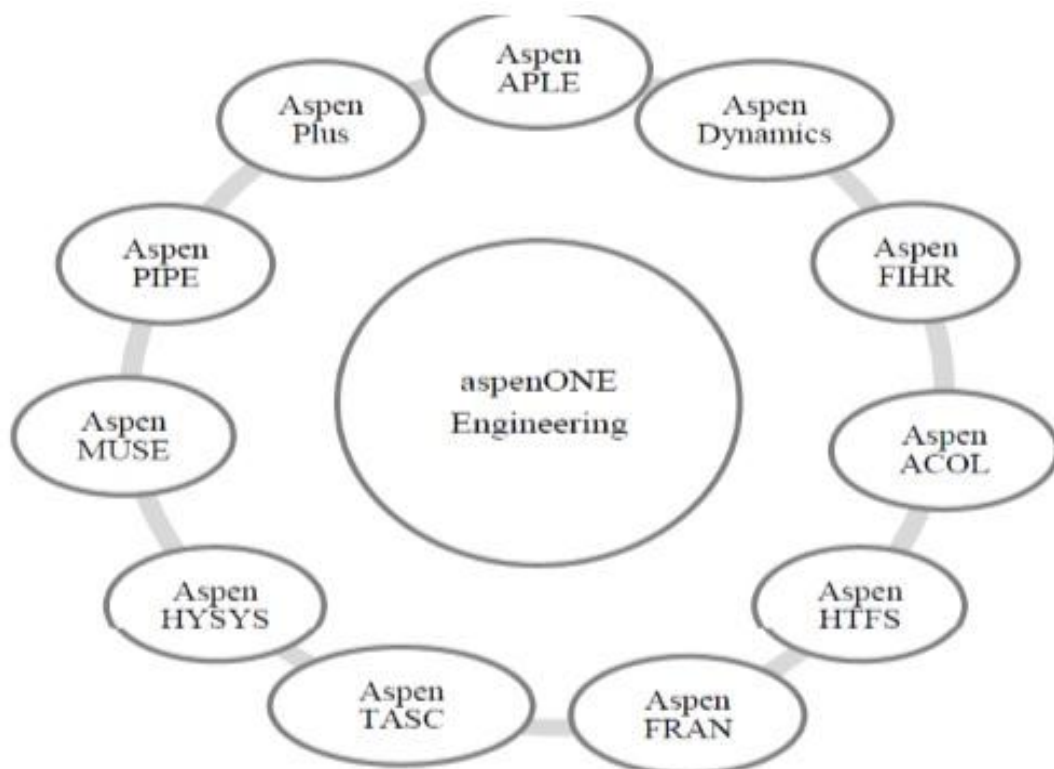

Fig 4.1: AspenONE engineering classifications.

4.2 FEATURES [18]

1. Aspen Plus incorporates the world's best-in-class database of phase equilibrium data for electrolytes, polymers, solids and conventional chemicals. The data is updated

on a regular basis by the United States National Institute of Standards and Technology (NIST).

2. Aspen Properties Mobile is also one of the features that enables us to access the data and the physical property calculations.

3. Aspen Plus is integrated with AspenTech's heat exchanger design software and cost analysis software. The proper integration of process simulations with costing and design software promotes more appropriate designs based on vast cost estimates and eliminates expensive manual iterations.

4. Equation Oriented Modelling (EOM) capability of Aspen Plus helps in simulating even the most complex and large scale processes.

5. Aspen Plus considers rate-based distillation which enables us to perform calculations involving distillation while monitoring other mass transfer operations.

6. Aspen Plus enables us to simulate batch distillation columns in a rigorous way.

7. Aspen Plus helps us in the identification of azeotropes.

8. Aspen Plus modelling results can be associated with Microsoft Excel® by the use of Aspen Simulation Workbook.

9. Aspen Dynamics is used for controllability and safety studies, optimizing transition, sizing relief valves, shutdown and start up policies.

4.3 SIMULATING ENVIRONMENT

The simulating environment comprises of the area where the flow sheet and most of the work such as defining and installing streams, unit operations, columns and sub flow sheets is done. The simulating area of Aspen Adsim is shown in Fig. 4.2.
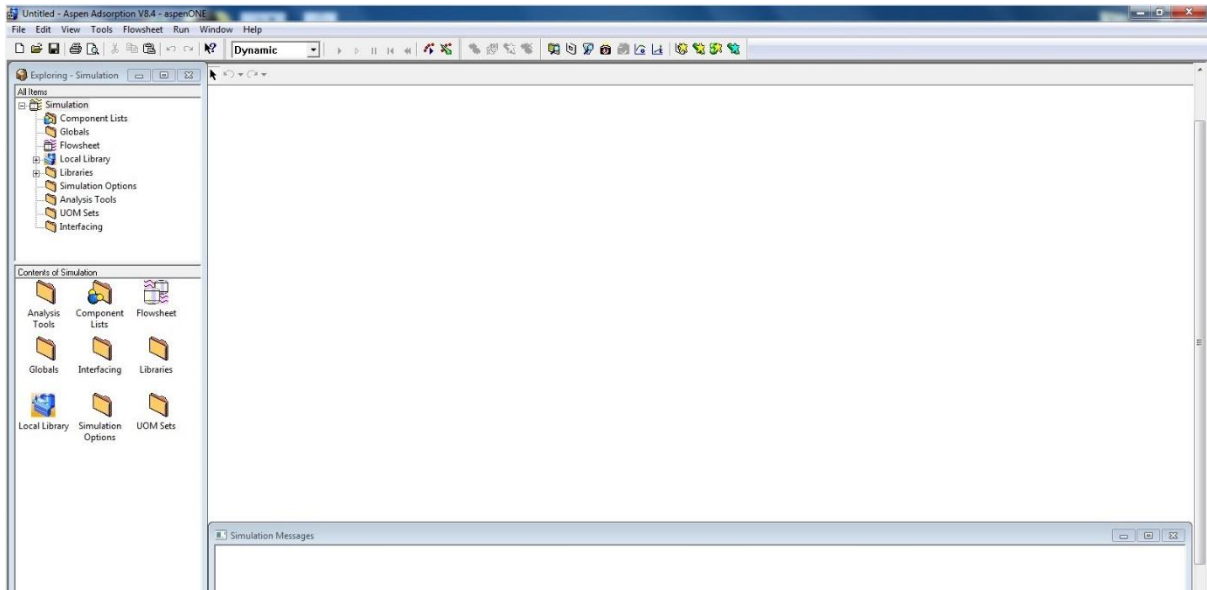
Fig 4.2: The simulation environment of Aspen Adsim.

Before the configuration of the flow diagram, specification of the input parameters such as nomenclature of the components, selection of the base method, etc. is done using the properties plus window as shown in Fig. 4.3. Here, the components (air and ethyl acetate) are added using the find tab.
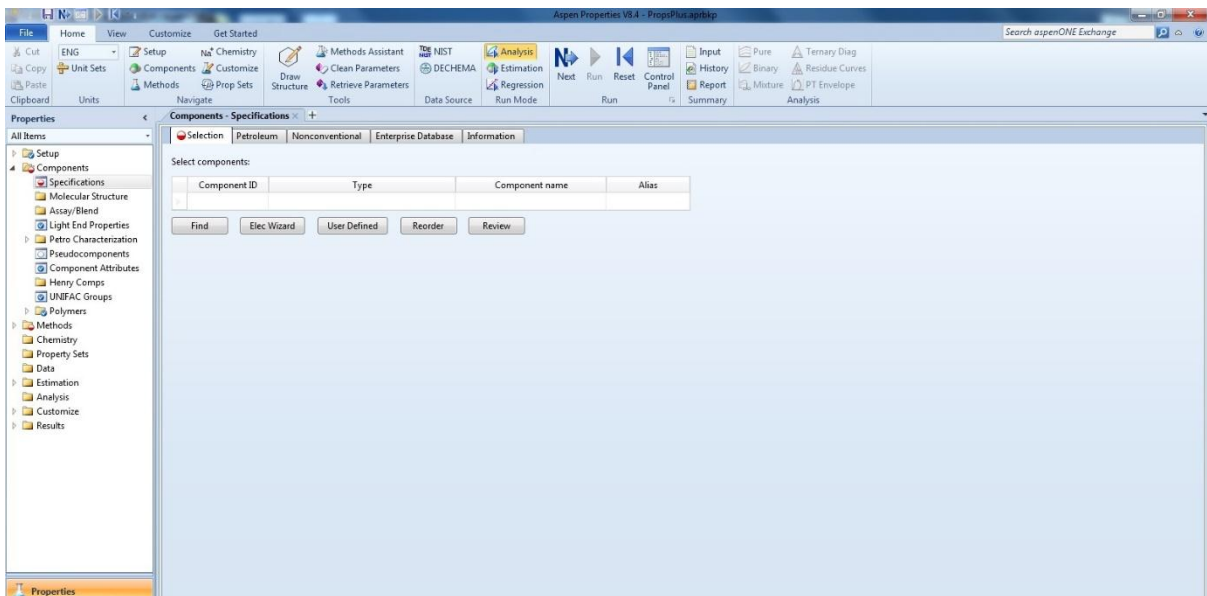
Fig 4.3: The properties plus window to specify components.

The base method window is shown in Fig. 4.4. Base method chosen for the simulations is Peng-Robinson method.

Fig 4.4: Specification of the base method (Peng-Robinson).

After the completion of the input parameters, the flow diagram of the adsorption process is drawn using the Gas Dynamic tab in Adsim library of Aspen Adsim. The specification of gas bed, gas feed and gas product is done afterwards.

Fig 4.5: Flowchart of the adsorption process.

CHAPTER – 5

RESULTS AND DISCUSSION

5. RESULTS AND DISCUSSION

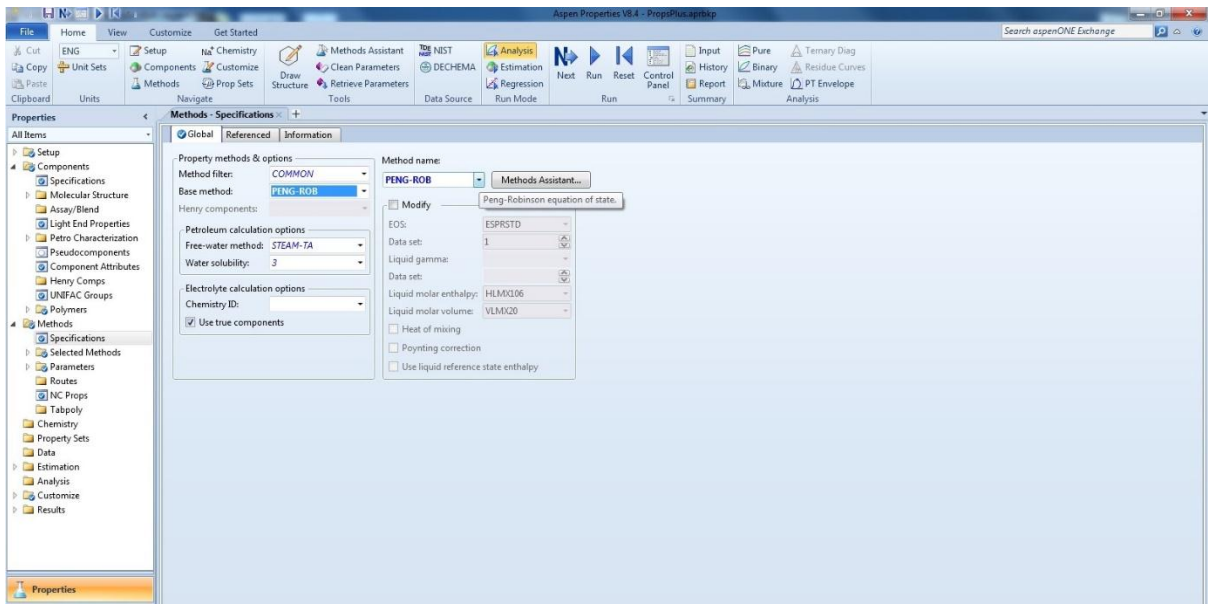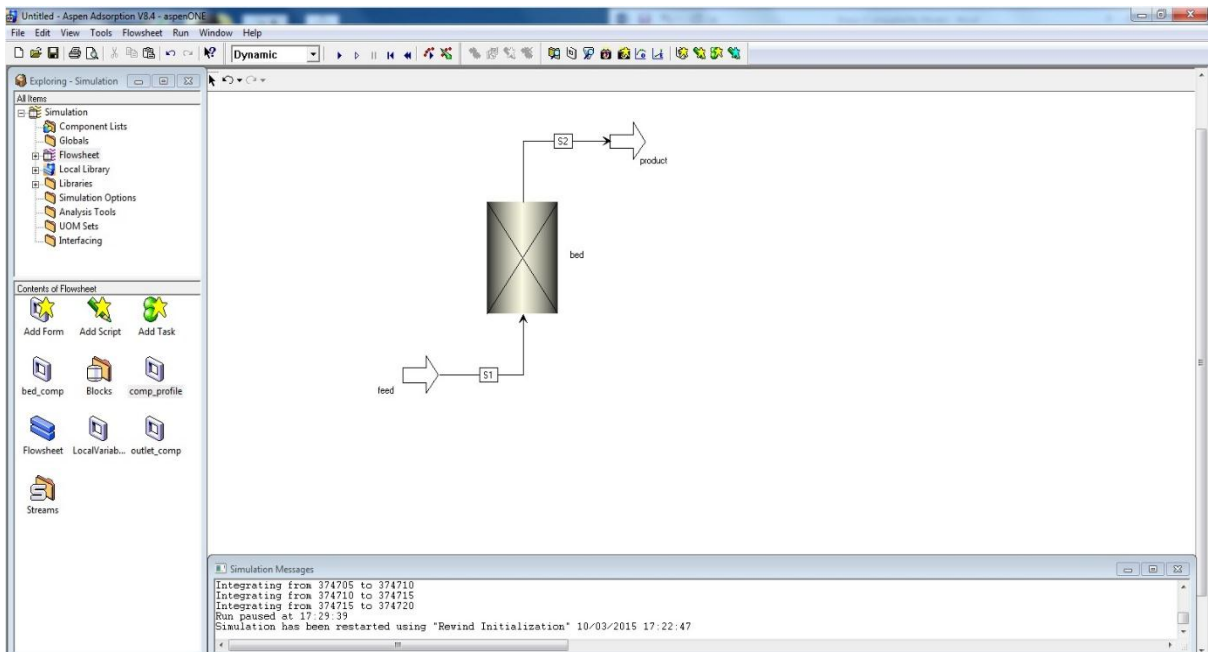Isothermal simulations were carried out for a set of inlet concentrations of ethyl acetate at three separate temperatures, 30. 45 and 55 °C. The Langmuir constant (b) and the saturation capacity (q_s), for ethyl acetate adsorption onto activated carbon depend on temperature. The values of Langmuir constant and saturation capacity for different temperatures are mentioned in Table 2. As it is clear from Table 2, saturation capacity decreases with rise in temperature because as the temperature rises the adsorption capacities reduce. The explanation for the reduction in saturation capacity with rise in temperature can be advocated by the point of difference between the original Langmuir formulations, where the saturation limit was considered as the saturation of a certain number of identical sites on the surface, and the current Langmuir formulations, where the saturation limit is corresponding to the saturation of the micropore volume. If the saturation limit is considered as the saturation of the micropore volume, a considerable decrease in the value of saturation capacity is usually witnessed with increase in temperature [13]. Variables studied in the packed-bed adsorption of ethyl acetate onto activated carbon from a mixture of air and ethyl acetate are temperature, inlet ethyl acetate concentration, bed height, flow velocity and overall mass transfer coefficient; and their range of study is mentioned in Table 3.

Table 3. Variables studied in ethyl acetate adsorption on activated carbon.

Variables	Range
T ; K	303 – 328
$v_o \times 10^3$; m/s	3.0 – 7.0
c_{in} ; kg/m^3	0.208 – 0.416
L ; m	0.06 – 0.10
k ; s^{-1}	0.1 – 500

The values of IP_1 and IP_2 used in the simulation process are obtained from the values given in Table 2 and the equations for IP_1 and IP_2 as mentioned in the modelling section. The calculated values of IP_1 and IP_2 are mentioned in Table 4.

Simulations are carried out in order to study the effect of changing variables on the dynamic adsorption behavior of ethyl acetate onto activated carbon. Results of the simulations are represented in the form of concentration breakthrough curves and the effect of the variables on them. The data for simulation and the input parameters of the experimental runs are shown in Table 6. The value are in consistence with the data provided in [15]. Once the breakthrough curve is consistent, the values of the variables are further changed to study the effect of the variables on the adsorption breakthrough curves.

Table 4: Values used of IP_1 and IP_2 for simulations

Temperature; к	$IP_1 = q_s b$ / M	$IP_2 = b$ / M
303	0.6859	0.9369
318	0.4525	0.7748
328	0.35568	0.73035

Table 5. Configuration of the adsorption bed.

Parameters	Configuration
Number of layers in bed	1
Bed type	Vertical
Spatial dimensions	1-D
Internal heat exchanger	None
Discretization method	UDS1
Number of nodes	20

Table 6. Values of Input parameters for simulation runs [2].

Parameters	Base values
Bed height; m	0.06
Bed Diameter; m	0.1
Average particle diameter; m	0.00158
Adsorbate molecular diffusivity; m²/s	8.9×10^{-6}
Inter particle voidage	0.4
Intra particle voidage	0.58
Inlet fluid temperature; K	318
Initial solid temperature; K	318
Solid density; kg/m³	500
Gas velocity; m/s	3×10^{-3}
Inlet EA concentration; kg/m³	0.312
Density of mixture; kg/m³	1.04
Molecular weight of mixture; kmol/kg	54.19321
q_s; kg/kg and b; m³/kg	0.584; 41.99
IP_1 and IP_2; m³/kg	0.4525; 0.7748

Data for the activated carbon, as shown in Table 1, used for the simulation runs was provided by E-Merck, India [15]. The activated carbon bed configuration chosen for the simulation runs is given in Table 5.

EFFECT OF TEMPERATURE

In the current study of concentration breakthrough curves, three distinct temperatures of 30, 45 and 55° C are taken in account.

The adsorption of ethyl acetate by activated carbon is controlled by the rate mechanisms mentioned below:

- o Bulk diffusion – Diffusion of bulk gas to the surface of activated carbon through a gas film surrounding the bed.
- o Pore diffusion – Diffusion of gas into the pores.
- o Surface reaction – Surface reactions involved in adsorption process are adsorption/desorption.

The plot of concentration breakthrough curves with changing temperature is given in Fig 5.1. As it is clear from the plot, the breakthrough time of the adsorption process starts decreasing with increase in the temperature. This means for higher temperatures the saturation of the activated carbon bed occurs in less time. The decrease in time of saturation is proportional to the increase in the temperature.
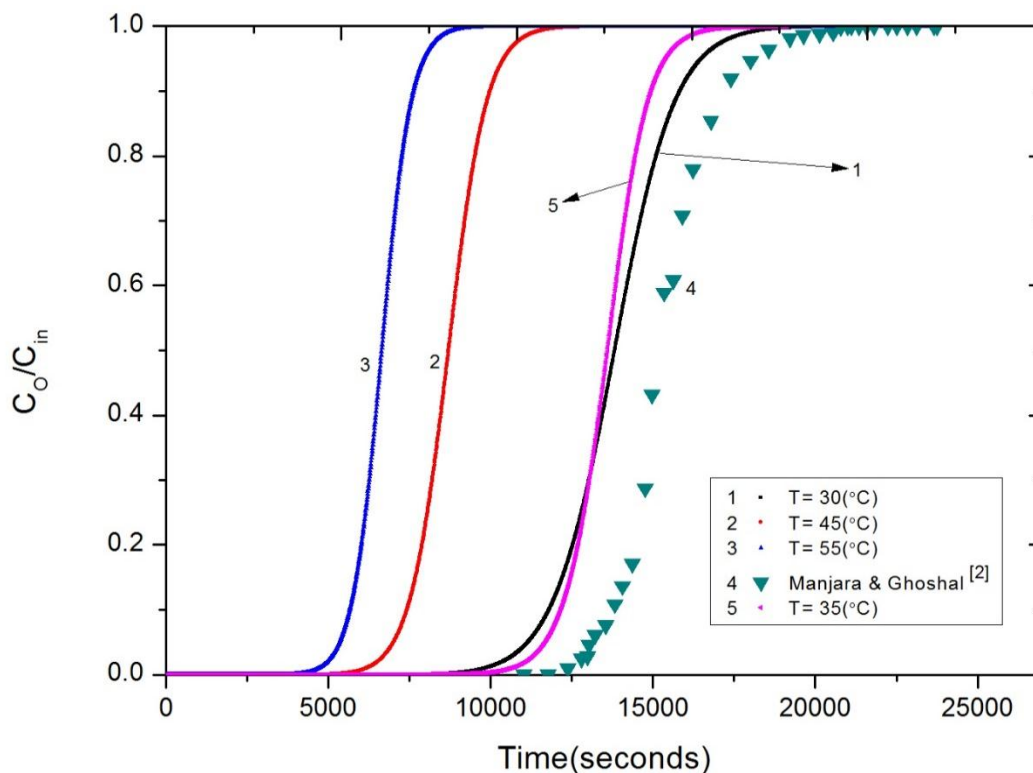

Fig 5.1: Effect of temperature on concentration breakthrough curves

In the above plot temperatures 30, 45 and 55° C are represented by curves 1, 2 and 3 respectively. As seen from the curves, with increase in temperature the breakthrough time of the adsorption process shifts towards left i.e. decreases. The curves 4, shown as data points, and 5 represent the experimental results taken from Manjare & Ghoshal [2] and the simulated results for the same set of data respectively. The values of temperature and inlet EA concentration considered in that study are 35° C and 0.450 kg/m^3 respectively. Curve 4 and curve 5 are in good agreement with each other. Values of inlet EA concentration for curve 1, 2 and 3 is 0.312 kg/m^3. With rise in temperature, not only the curve shifts towards left, it also becomes steeper. This means that with increase in temperature, rate of saturation also increase.

EFFECT OF INLET EA CONCENTRATION

Three distinct variations of inlet ethyl acetate concentration are studied in this section. Values chosen for the simulations are 0.208, 0.312, and 0.416 kg/m^3. The inlet VOC concentration has a peculiar effect on the concentration breakthrough curves. As we start increasing the inlet EA concentration, the breakthrough time of the curve increases whereas the saturation time of the curve decreases.

The effect of inlet EA concentration on concentration breakthrough curve is shown in Fig. 5.2. The above discussed results can easily be spotted on the curve. As we see here, with increasing inlet EA concentration, the curve move towards the right near in the lower half of the plot whereas in the upper part of the plot with increase in inlet EA concentration, the curve moves towards left resulting an overall less time interval for the saturation of the activated carbon bed.
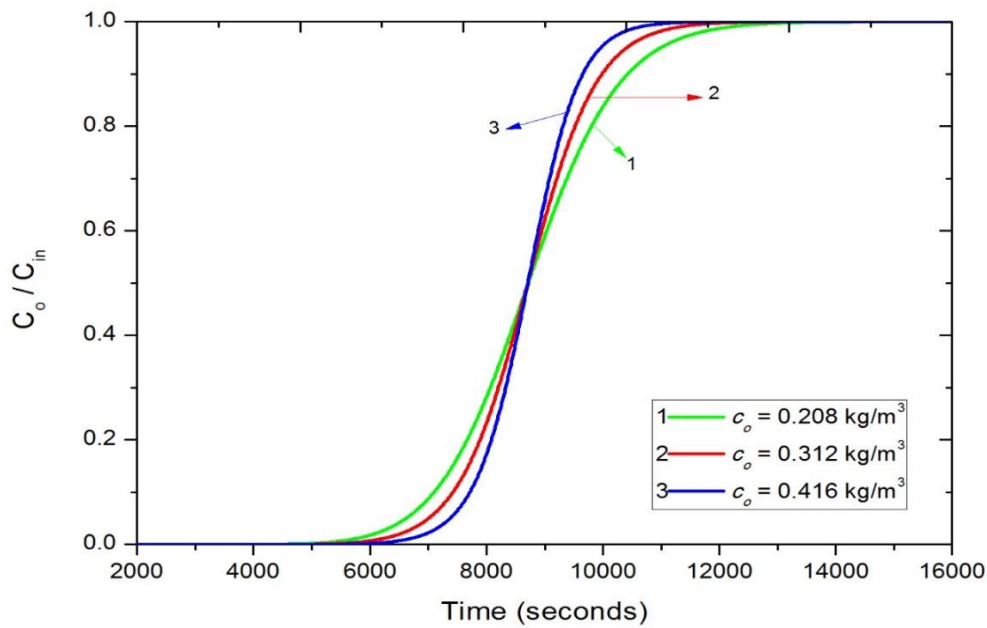
Fig 5.2: Effect of inlet EA concentration on concentration breakthrough curves

There is a point of inflexion in the curve where all the different concentration plots seem to cross each other and possess approximately the same value.

The decrease in the saturation time and increase in the breakthrough time simply indicates less time for saturation. In other words, as we increase the inlet VOC concentration, the time of saturation in decreased which in turn results in an increased rate of saturation. So it is safe to state that with increase in inlet EA concentration the rate of saturation increases.

EFFECT OF INLET GAS VELOCITY

The distinct values chosen to study the effect of inlet gas velocity on the concentration breakthrough curves are 3×10^{-3}, 5×10^{-3} and 7×10^{-3} m/s. It is clear from the plot that as we increase the inlet gas velocity the curve shifts towards left i.e. decrease in the breakthrough time and saturation time of the curve. Also with decrease in the inlet gas

velocity the curve becomes steeper. The increase in steep of the curve indicates the increase in the rate of saturation.

In Fig 5.3 the three different velocities are shown by curves 1, 2 and 3 respectively. Plot 1, the curve for lowest velocity, is in the most right position and as the gas velocity increases the curve starts shifting towards left with plot 3, the curve for the highest velocity, being in the most left and line 2 is placed between the two.
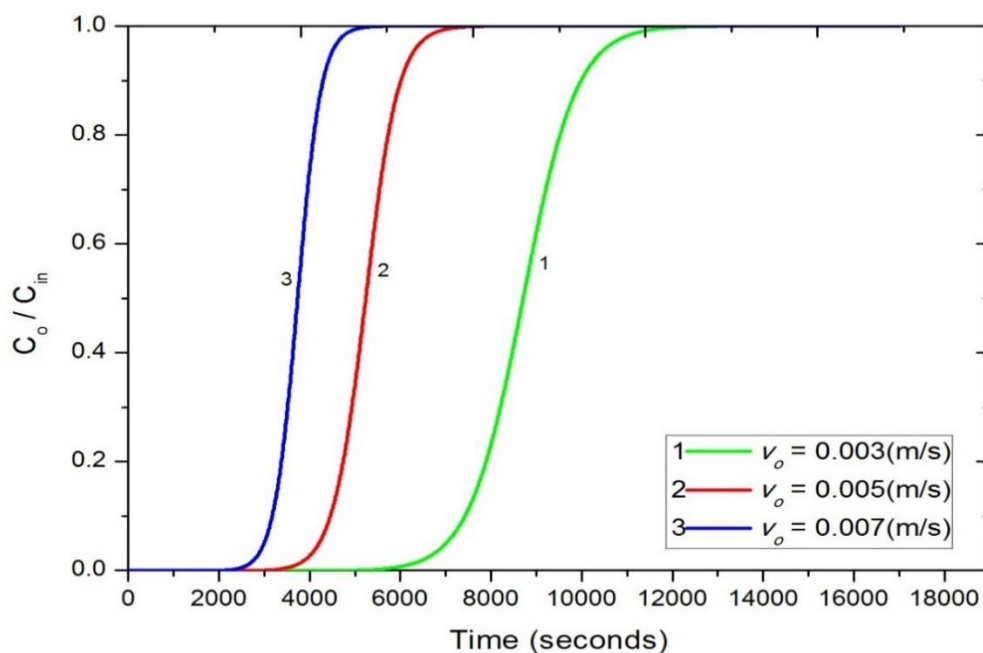
Fig 5.3 Effect of inlet gas velocity on concentration breakthrough curves.

In general as we increase the inlet gas velocity, the adsorption of the VOC reduces as the kinetic energy of the VOC molecules increase. This is due to the fact that in most of the adsorbents, the adsorption takes place at the surface. In case of activated carbon, the porosity is very high and most of the adsorption takes place inside the pores. So as we increase the kinetic energy, we also increase the probability of the molecules entering the pores and get adsorbed and hence the breakthrough time decreases.

EFFECT OF ADSORPTION BED HEIGHT

As it can be easily inferred from the plot given below, with increase in the bed height, the breakthrough time and the saturation time of the curves increase. This change in the adsorption behaviour can be explained by the simple fact that for taller adsorption beds the availability of the micropore volume in the bed is more than that in the smaller adsorption beds. Due to this difference in micropore volume of the beds, the time taken for the complete saturation of the beds are different. As the bed height increases the micropore volume increases and hence to saturate a larger micropore volume longer time is required.

The effect of adsorption bed height on the concentration breakthrough curves is shown in Fig 5.4. The values chosen for the simulation of experimental runs are 0.06, 0.08 and 1.0 m. The curves representing the above mentioned values are curve 1, 2 and 3 respectively.
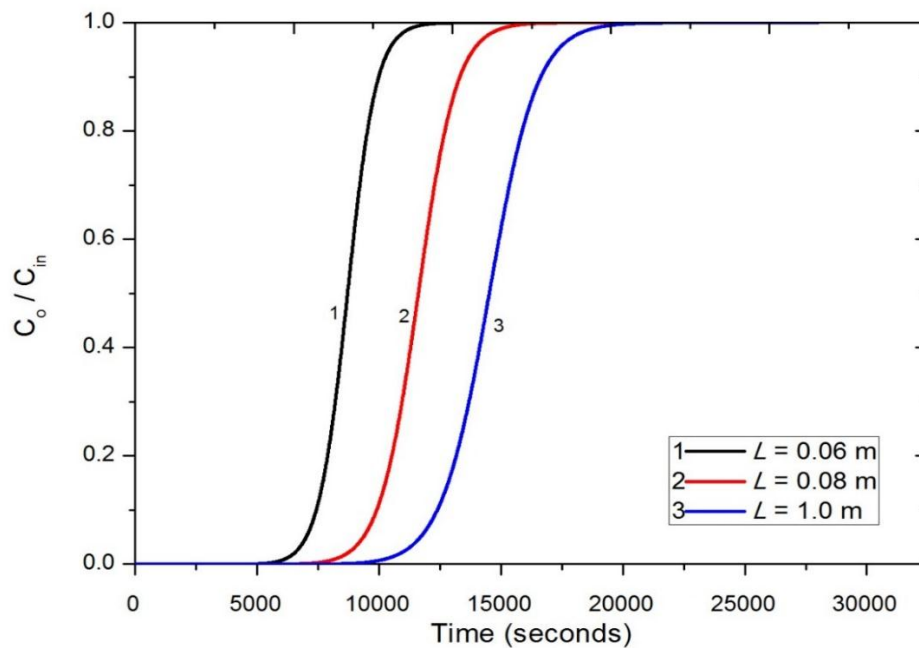

Fig 5.4: Effect of adsorption bed height on concentration breakthrough curves.

EFFECT OF OVERALL MASS TRANSFER COEFFICIENT

The distinct values of overall mass transfer coefficients chosen for the simulation runs are obtained from equation 12. The base value of overall mass transfer coefficient was found to be 141.18 s^{-1} using the values of diffusivity and the particulate radius from table 5. The nature of the plot with changing mass transfer coefficient is shown in Fig 5.5.
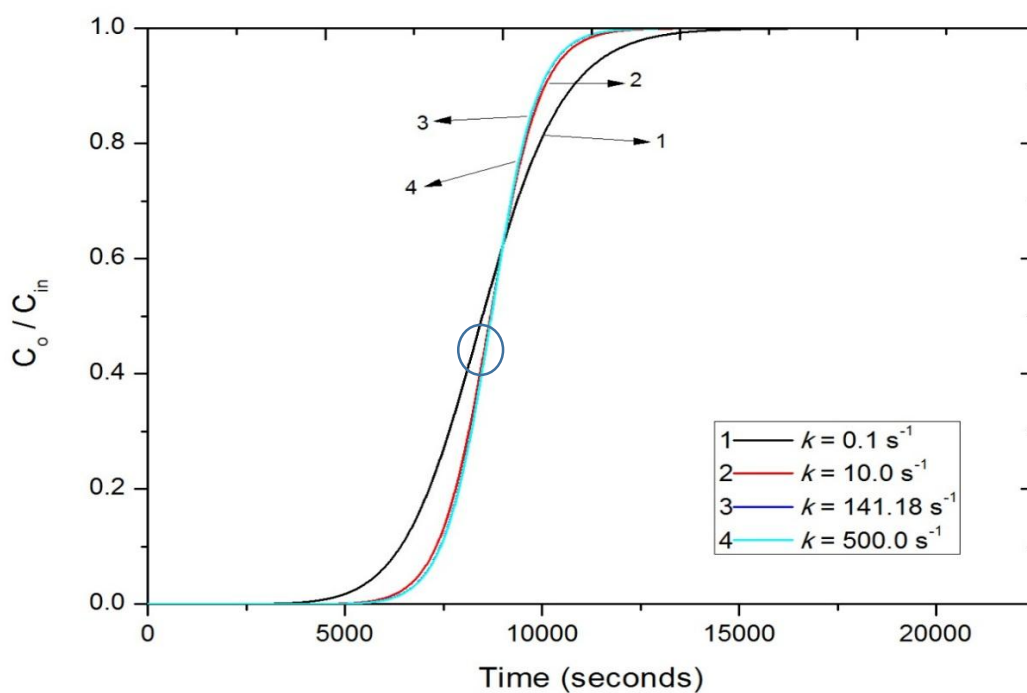

Fig 5.5 Effect of overall mass transfer coefficient on concentration breakthrough curves

The four distinct values of overall mass transfer coefficients represented by curve 1, 2, 3 and 4 are 0.1, 10.0, 141.18, and 500 s^{-1} respectively. For smaller values of MTC the change in breakthrough time and saturation time is considerable and can be seen on the plot easily. As we increase the MTC values, the curves start getting close and converge after a certain value. In Fig 5.5, curve 2 is very close to the coinciding curves 3 and 4. For curves 3 and 4 the MTC values chosen are 141.18, and 500 s^{-1} respectively. Despite the difference in the values, the

curves are coinciding. In order to show the convergence of the curves, a small encircled section in Fig 5.5 is zoomed in and shown in Fig 5.6.
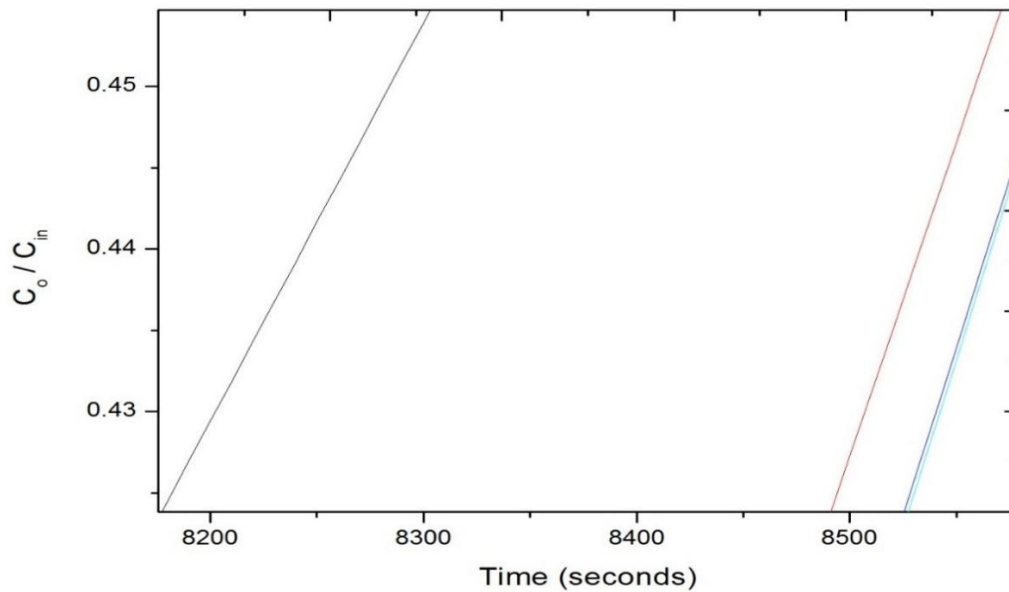

Fig 5.6 The encircled part in Fig 5.5 zoomed in to show the vicinity of the curves

As the curve in Fig 5.5 clearly shows, with increase in the overall mass transfer coefficient the breakthrough time of the curve increases whereas the saturation time of the curve decreases. The nature of the curve is quite similar to that of the Fig 5.2. Another very important thing to notice is that as we increase the overall mass transfer coefficient the curves start to converge. This means for higher values of MTC the curves will be overlapping.

Increase in breakthrough time and decrease in saturation time corresponds to the increased rate of saturation. So it is suffice to say, with increase in the overall MTC value the rate of saturation increases. From Fig 5.6 it is clear that as we go on increasing the MTC value, the increment in the rate of saturation starts decreasing and becomes very small after a certain value. As a result of that for higher value of overall mass transfer coefficient, the rate of saturation is approximately constant.

CHAPTER – 6

CONCLUSION

6. CONCLUSION

This thesis shows the modelling of breakthrough curves of ethyl acetate on granular activated carbon. The simulations have been carried out with changing values of variables such as temperature, inlet EA concentration, bed height, overall mass transfer coefficients and inlet gas velocity. The results obtained from the simulations infer that activated carbon is an effective adsorbent for the dynamic adsorption of ethyl acetate for smaller concentrations. The results of the simulations are in agreement with the data chosen from Manjare and Ghoshal [2]. The Langmuir parameters of the activated carbon indicate a good adsorption capacity to remove VOCs. The simulation results show that the adsorption process is best favoured when the inlet temperature is high and the inlet ethyl acetate concentration is low (preferably in ppm range). Micropore volume of the activated carbon, a very essential factor affecting the adsorption dynamics, depends on two important factors: microporosity and bed height. Increasing the microporosity of the adsorption bed increases the period of time for which the adsorption occurs, the breakthrough time is larger as compared to that of low microporosity adsorption beds. Bed height also influences the micropore volume. For a fixed microporosity, the adsorption bed with more height will possess a higher micropore volume. This fact is justified in Fig 5.4 where, with increase in the bed height the breakthrough time increases as a result of increase in the micropore volume.

Nomenclature

a_p = adsorbent surface area per unit adsorbent volume; m^2/m^3

b = Langmuir constant; m^3/kg

b_o = pre-exponential factor in van't hoff equation; m^3/kg

c_o = outlet concentration of EA; kg/m^3

c_{in} = inlet EA concentration in the fluid phase; kg/m^3

q^* = equilibrium adsorption amount; kg/kg

q = adsorbed amount at any time; kg/kg

q_s = adsorbent saturation capacity; kg/kg

k = mass transfer coefficient; s^{-1}

v_o = superficial gas velocity; m/s

D_e = effective diffusivity; m^2/s

w_i = solid loading; kmol/kg

IP_1 = aspen isothermal parameter 1

IP_2 = aspen isothermal parameter 2

M = molar molecular weight of the inlet gas mixture; kg/kmol

L = length of the bed; m

P = pressure; bar

T = temperature; K

$-\Delta H$ = heat of adsorption; J/kg

h = HTC between gas and solid; kJ/s.m^2.K

Q = flowrate; kmol/hr

R_p = radius of the particle; m

t = time; s

Greek Symbols:

ε = bed porosity

ρ = density; kg/m^3

Subscripts and Superscripts:

Δ = gradient

in = inlet condition

o = outlet condition

b = bed

g = gas

p = pellet

s = solid

REFERENCES

[1] Bansal R.C., Goyal M, *Activated Carbon Adsorption*, Taylor & Francis group, Florida, 2005.

[2] Manjare, Sampatrao D., Ghoshal A. K, "Studies on Adsorption of Ethyl Acetate Vapor on Activated Carbon", Ind. Eng. Chem. Res. 2006, 45, 6563-6569

[3] Faisal I. Khan, Aloke Kr. Ghoshal, "Removal of Volatile Organic Compounds from polluted air", Journal of Loss Prevention in the Process Industries 13 (2000) 527–545

[4] Ruddy, E. N., & Carroll, L. A. (1993). Select the best VOC control strategy. *Chemical Engineering Progress*, *7*, 28 July.

[5] USEPA (1991). EPA handbook: *control technologies for hazardous air pollutants* USEPA: Office of Research and Development, Washington D.C., 1991.

[6] Pezolt, D. J., Collick, S. J., Johnson, H. A., & Robbins, L. A. (1997). Pressure swing adsorption for VOC recovery at gasoline terminals. *Chemical Engineering Progress*, *16* (1), 16.

[7] Mattson JS and Mark HB, Jr. Activated carbon. New York: *Dekker*. 1971

[8] Jufang Wu, Modeling adsorption of organic compounds on activated carbon — a multivariate approach, Umeå University, SE-901 87 Umeå, Sweden, Division of NBC Defence, SE-901 82 Umeå, Sweden, 2004.

[9] Sing KSW, Everett DH, Haul RAW, Moscou L, Pierotti RA, Rouquerol J, Siemieniewska T. Reporting physisorption data for gas/solid systems with special reference to the determination of surface area and porosity. *Pure & Appl Chem* 57(4):603-19. 1985.

[10] Kenny MB, Sing KSW, Theocharis C. In: Proc. 4th Int. Conf. On Fundamentals of adsorption (Suzuki M, editor), Kodansha, Tokyo, p 323. 1993.

[11] Kaneko K. In: Equilibria and Dynamics of Gas Adsorption on Heterogeneous Solid Surfaces (Rudinski W, Steele WA and Zgrablich G, editors). *Elsevier*, Amsterdam, p 679. 1997

[12] Cheremishinoff NP and Moressi AC. Carbon adsorption applications, in Cheremishinoff NP and F Ellerbusch (EDS.) *Carbon Adsorption Handbook*: 1-53. Ann Arbor: Ann Arbor Science. 1978.

[13] Manjare, S. D.; Ghoshal A. K, "Comparison of Adsorption of Ethyl Acetate on Activated Carbon and Molecular Sieves 5A and 13X", J. Chem. Eng. Data 2006, 51, 1185-1189, India, 2006

[14] Aspen Adsim 2004, Adsorption Reference Guide, Version Number: 2004, November 2004

[15] Bird, R.B., Stewart, W.E., Lightfoot, E.N., *Transport Phenomena*, John Wiley and Sons, New York, 1960.

[16] Ruthven, D. M. *Principles of Adsorption and Adsorption Processes*; Wiley: New York, 1984.

[17] C Yang, R. T. Gas Separation by Adsorption Processes; *Butterworth*: Boston, 1987

[18] Aspentech Aspen Plus: http://www.aspentech.com/core/aspen-plus.aspx

[19] Manjare, S. D.; Ghoshal A. K, "Adsorption Equilibrium Studies for Ethyl Acetate Vapour and E-merck 13 X Molecular Sieve System", *Elsevier*, Sep. Purif. Technol. 51 (2006) 118-125, India, 2006, in press, doi: 10.1016/j.seppur.2006.01.004.

[20] Das D., Gaur V., Verma N., "Removal of volatile organic compound by activated carbon fiber", *Carbon 42* (2004) 2949–2962, India, 2004.